Paper 282

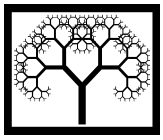

Proceedings of the Eleventh International Conference
on Computational Structures Technology,
B.H.V. Topping, (Editor),
Civil-Comp Press, Stirlingshire, Scotland

Finite Element Analyses of Reinforced Concrete Beams Strengthened using CFRP

A.E. Demirer[1] and G. Arslan[2]
[1]Department of Civil Engineering
[2]Institute of Science & Technology
Yıldız Technical University, Istanbul, Turkey

Abstract

In this paper, finite element plastic analyses of reinforced concrete (RC) beams strengthened by carbon fibre reinforced polymers (CFRP) were performed considering flexural capacity. Three-dimensional finite element analyses (FEA) of beams with different geometrical and material properties, which are available in the literature, were conducted. The properties of the beams in the nonlinear finite element model are the same as those of the actual beams. Observing that the experimental and numerical load-deflection curves are consistent, the strains in the CFRP obtained through FEA were compared with the predictions by ACI 440 [1]. It is observed that the results of FEA agree with the strains predicted using the ACI 440 equation.

Keywords: fibre reinforced polymer, retrofitting, reinforced concrete, beam, finite element, flexural.

1 Introduction

Reinforced concrete (RC) structural elements may need structural strengthening for several reasons, such as design and implementation errors, time-dependent degradations, change of intended use and modifications in structural codes. In last three decades, structural retrofitting using fibre reinforced polymers (FRP) has increased [2-6], because of their advantages such as high strength and durability, being a noncorrosive material, easy application and negligible increase in cross-sectional dimensions and weight of structural members. An increase by 10% to 160% in the flexural strength of RC beams is observed by attaching FRP laminates, oriented along the length of the beam, to the tension face of the beam [7-9]. However, an increase up to 40% is acceptable considering strengthening limitations, ductility and serviceability limitations [1].

In this study, finite element plastic analyses of RC beams strengthened by CFRP were performed considering flexural capacity. The finite element plastic analyses of a number of RC beams with different geometrical and material properties, which are available in the literature, were conducted. Finite element analyses (FEA) using the ANSYS 11.0 [10] were performed to determine the flexural strength of strengthened RC beams with CFRP, which a perfect bond between concrete and reinforcement, and concrete and CFRP is assumed. Observing that the experimental and numerical load-deflection curves are consistent [11], the strains in the CFRP obtained through FEA were compared with the predictions by ACI 440 [1]. It is observed that the results of FEA agree with the strains predicted using the ACI 440 equation.

2 Flexural Capacity of Beams According to ACI 440

The major factors affecting the failure load after debonding of FRP are: (i) the concrete compressive strength; (ii) the orientation of cracks in the load span; (iii) the width and the extent of cracks; (iv) the ratio of transverse reinforcement and (v) FRP configurations. To account for the factors above, the design flexural capacity must equal or exceed the flexural demand (Eq. (1)). The nominal moment capacity should be computed with the load factors according to ACI 318 [12].

$$\phi M_n \geq M_{ult} \tag{1}$$

in which ϕ is the moment reduction factor, M_n is the nominal moment capacity and M_{ult} is the ultimate moment capacity of RC beams strengthened with FRP. A few models have been proposed in order to calculate the ultimate flexural strength of the RC beams strengthened with FRP. In this study, the ultimate strain and load-carrying capacity obtained by FEA were compared with the predictions using ACI 440 [1] model.

According to ACI 440 [1], if the strain in the FRP reaches the design rupture strain, $\varepsilon_f = \varepsilon_{fu}$, before the concrete reaches the maximum usable strain, the FRP will rupture. The rupture strain value may be given by the FRP manufacturer. If not, the following equation can be used to calculate the rupture strain:

$$\varepsilon_{fu} = \frac{f_{fu}}{E_f} \tag{2}$$

in which f_{fu} and E_f are the ultimate tensile strength and modulus of elasticity of the FRP, respectively.

If the RC system cannot support the force in the FRP, FRP debonding or cover delamination is a possibility. At the end of the FRP sheet, intermediate crack-induced debonding may be the controlling failure. In order to prevent this type of failure, ACI 440 [1] limits the effective strain level in the FRP to the strain level where debonding may occur:

$$\varepsilon_{fd} = 0.41\sqrt{\frac{f_c}{nE_f t_f}} \leq 0.9\varepsilon_{fu} \tag{3}$$

in which f_c is concrete compressive strength, n is number of FRP layers, and t_f is FRP layer thickness.

According to ACI 440 [1], when calculating the strains in the FRP sheets, the initial strain in the concrete system has to be considered. The initial strains are a result of the self-weight of the system and any pre-stressing forces that may be present. These initial strains must be excluded from the strain calculated for the strains in the FRP. An elastic analysis based on cracked section properties should be used to find the initial strains in the system. The initial strain in the concrete is defined as:

$$\varepsilon_{bi} = \frac{M_{DL}\left(d_f - kd\right)}{I_{cr}E_c} \tag{4}$$

in which M_{DL} is the dead load moment, d_f is effective depth of FRP, d is distance from extreme compression fibre to center of tensile reinforcement, k is the ratio of depth of neutral axis to reinforcement depth measured from extreme compression fibre, I_{cr} is the cracked moment of inertia transformed to concrete, and E_c is the modulus of elasticity of concrete.

The strain developed in the FRP, at the point when concrete crushes, the FRP ruptures, or the FRP debonds, determines the maximum strain that can be obtained in the FRP sheets. The effective strain level in the FRP at the ultimate state is defined as

$$\varepsilon_{fe} = \varepsilon_{cu}\left(\frac{d_f - c}{c}\right) - \varepsilon_{bi} \leq \varepsilon_{fd} \tag{5}$$

in which ε_{cu} is the maximum usable strain of concrete and c is the neutral axis depth. Once the strain is calculated, it can be used to calculate the stress level in the FRP by using the following equation:

$$f_{fe} = E_f \varepsilon_{fe} \tag{6}$$

in which E_f is the modulus of the FRP.

The initial strain in the steel and strain in the concrete compression is defined as

$$\varepsilon_s = \left(\varepsilon_{fe} + \varepsilon_{bi}\right)\left(\frac{d - c}{d_f - c}\right) \tag{7}$$

$$\varepsilon_c = \left(\varepsilon_{fe} + \varepsilon_{bi}\right)\left(\frac{c}{d_f - c}\right) \tag{8}$$

The stress in the steel can be calculated after the strain in the steel is calculated as:

$$f_s = E_s \varepsilon_s \le f_y \tag{9}$$

in which E_s and f_y are the modulus of elasticity and yield strength of the steel. The neutral axis depth can be found as:

$$c = \frac{A_s f_s + A_f f_{fe}}{\alpha_1 f_c \beta_1 b} \tag{10}$$

in which A_s is the area of the steel reinforcement, A_f is the area of the FRP, β_1 and α_1 is the parameter of stress block depth, ψ_f is FRP strength reduction factor, and b is width of a rectangular cross-section.

β_1 and α_1 are defined as

$$\beta_1 = \frac{4\varepsilon_{co} - \varepsilon_c}{6\varepsilon_{co} - 2\varepsilon_c} \tag{11}$$

$$\alpha_1 = \frac{3\varepsilon_{co}\varepsilon_c - \varepsilon_c^2}{3\beta_1 \varepsilon_{co}^{\ 2}} \tag{12}$$

in which ε_{co} is strain of concrete at the peak stress and can be calculated as

$$\varepsilon_{co} = \frac{1.7 f_c}{E_c} \tag{13}$$

The following equation can be used to calculate the ultimate flexural strength of the FRP strengthened RC system:

$$M_n = A_s f_s \left(d \frac{\beta_1 c}{2}\right) + \psi_f A_f f_{fe} \left(h \frac{\beta_1 c}{2}\right) \tag{14}$$

in which ψ_f is FRP strength reduction factor and h is height of the beam. Once the ultimate flexural strength of the beam is calculated, the ultimate load can be found by setting the ultimate moment equal to the maximum moment of the section and solving for the ultimate load.

3 Finite Element Modelling of RC Beams

Several studies have been performed numerically and experimentally during the last three decades in the field of strengthened RC beams in order to explain the stress distributions and failure modes [13]. Numerical investigations within the scope of this study were carried out using the finite element software ANSYS v11.0. Reinforcements and CFRP were modeled discretely using Link8 and Solid46 elements, respectively. Solid45 elements were used at the supports and at the loading regions to prevent stress concentrations. The concrete were modelled using Solid65 eight-node brick element, which is capable of simulating the cracking and crushing behavior of brittle materials. The Solid65 element requires linear isotropic and multiaxial isotropic material properties to model the concrete properly. The complete stress–strain curve model proposed by Mander et al. [14] was used. A full bond is assumed between concrete and reinforcement, and concrete and CFRP. A load-controlled analysis was performed by increasing the load at the tip of the beams incrementally. Only the half of the beam was modelled due to the symmetry of the loading and geometry. The analysis was carried out using the Newton-Raphson technique. The tensile strength of concrete, f_t, was taken as $0.3 f_c^{2/3}$ [15-16].

Experimental data were obtained from the existing sources of RC beam test results. Geometrical and material properties required for the modeling of the RC beams strengthened by CFRP are given in Table 1.

Series	Beam	$n\Phi_s$	$n\Phi_{sc}$	Φ_{sw}/s	n_f x t_f	L_o (mm)	L_p (mm)
B[a]	B0	2Φ16	2Φ10	Φ6/102	---	---	---
	B1	2Φ16	2Φ10	Φ6/102	1x2	381	2134
	B2	2Φ16	2Φ10	Φ6/102	1x2	305	2286
	B3-B4	2Φ16	2Φ10	Φ6/102	1x2	76	2744
	B5	2Φ16	2Φ10	Φ6/102	2x2	381	2134
	B6	3Φ16	2Φ10	Φ6/102	2x2	381	2134
S[b]	S0	3Φ12	3Φ12	Φ10/125	---	---	---
	S1	3Φ12	2Φ12	Φ6/125	2x0.13	150	2000
	S2	3Φ12	2Φ12	Φ6/90	2x0.13	150	2000
	S3	2Φ12	2Φ12	Φ6/125	2x0.13	150	2000

[a] Dong et al. [17]; [b] Pham and Al-Mahaidi [18]
$n\Phi_s$: number of tension steel bars·bar diameter (mm), $n\Phi_{sc}$: number of compression steel bars·bar diameter (mm), Φ_{sw}/s: transverse reinforcement diameters (mm) / spacing (mm), n_f x t_f: number of plies x ply thickness (mm), L_o: distance from end of CFRP to nearest support, L_p: CFRP length.

Table 1: Properties of the RC beams strengthened by CFRP.

Dong et al.'s [17] beams were tested in four-point bending with the span of 2900 mm and the shear span of 991 mm (Fig. 1, Table 2). The longitudinal steel

reinforcement consists of 10 mm and 16 mm diameter Grade 60 standard rebars having a yielding strength of 410 MPa. Concrete compressive strength of B series beams are 38.2 MPa. The transverse reinforcement consists of 6 mm diameter Grade 40 smooth bars. The beams are 152 / 305 mm in cross section, having a nominal tension steel depth of 253 mm. The CFRP fabric widths are 152 mm.

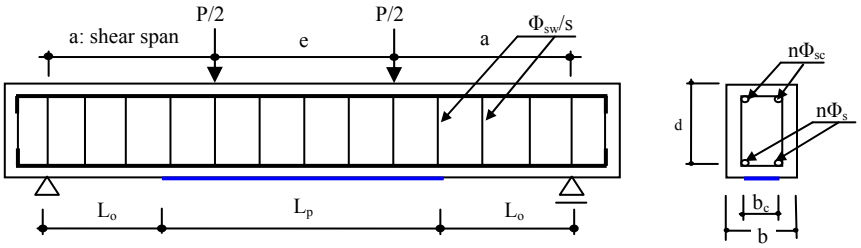

Figure 1: Details of RC beam strengthened by CFRP fabric.

Pham and Al-Mahaidi's [18] beams were tested in four-point bending with the span of 2300 mm and the shear span of 700 mm (Fig. 1, Table 2). The longitudinal steel reinforcement consists of 10 mm and 12 mm diameter rebars having a yielding strength of 334 and 504 MPa, respectively. The S group beam was retrofitted with 2 layers of CFRP. The concrete compressive strength for S0 beam is 47.7 MPa and S1-3 beams are 53.7 MPa, respectively. The beams are 140 / 260 mm in cross section, having a nominal tension steel depth of 220 mm. The CFRP fabric widths are 100 mm.

Series	Beam	a (mm)	b_c (mm)	b (mm)	d (mm)	e (mm)
B[a]	B0	991	---	152	253	914
	B1	991	152	152	253	914
	B2	991	152	152	253	914
	B3-B4	991	152	152	253	914
	B5	991	152	152	253	914
	B6	991	152	152	253	914
S[b]	S0	700	---	140	220	900
	S1	700	100	140	220	900
	S2	700	100	140	220	900
	S3	700	100	140	220	900
[a] Dong et al. [17]; [b] Pham and Al-Mahaidi [18]						

Table 2: Details of RC beams strengthened by CFRP.

4 The Results of FEA

4.1 Comparison of Load–Deflection Curves

As shown in Table 3, the mean value (MV) of the ratio of the experimental (Exp.) load-carrying capacity to the results of FEA and the standard deviation (SD) are 1.08 and 0.07 for all beams, respectively. The MV of the ratio of the experimental deflection capacity to the results of FEA and the SD are 0.90 and 0.15 for all beams, respectively. Most of the deflection values obtained from FEA are smaller than the test results, due to the perfect bond assumption between concrete and steel bars, and concrete and CFRP.

Beam	Ultimate load			Ultimate deflection		
	$P_{u,Exp.}$ (kN)	$P_{u,FEA}$ (kN)	$\frac{P_{u,Exp.}}{P_{u,FEA}}$	$\delta_{u,Exp.}$ (mm)	$\delta_{u,FEA}$ (mm)	$\frac{\delta_{u,Exp.}}{\delta_{u,FEA}}$
B0	96.59	100.00	1.04	70.17	53.55	0.76
B1	148.20	165.00	1.11	31.86	22.37	0.70
B2	157.95	177.00	1.12	24.31	26.24	1.08
B3-B4	188.05	201.08	1.07	34.70	34.72	1.00
B5	178.40	203.50	1.14	20.40	21.34	1.05
B6	181.72	220.00	1.21	20.97	17.85	0.85
S0	108.25	108.75	1.00	41.43	26.34	0.64
S1	148.25	151.20	1.02	28.00	27.53	0.98
S2	154.85	154.19	1.00	28.55	27.81	0.97
S3	120.45	128.00	1.06	32.00	29.58	0.92
		MV	1.08		MV	0.90
		SD	0.07		SD	0.15

Table 3: Comparison of experimental and numerical results.

The load versus deflection curves obtained through FEA are plotted in Fig. 2, together with the experimental results. It is observed that there is a good agreement with the numerical and experimental results. Comparing the ultimate load capacity, the FEA results of strengthened beams was found to be 1.00~1.21 times the corresponding experimental results, where the MV is 1.08. As the distance from the end of CFRP to the nearest support decreases, the load-carrying capacity increases. Similarly, mid-span deflection increases with the distance from the end of CFRP to the nearest support (B1, B2, B3-4 beams).

It can be said that load-deflection curves obtained experimentally and numerically are in good agreement up to the formation of first crack, but the ones obtained numerically exhibit a more rigid behaviour in the region enclosed by the formation of first crack and the yielding of tensile reinforcement. It is concluded that this rigid behaviour is a result of the perfect bond assumption between concrete and steel bars and concrete and CFRP.

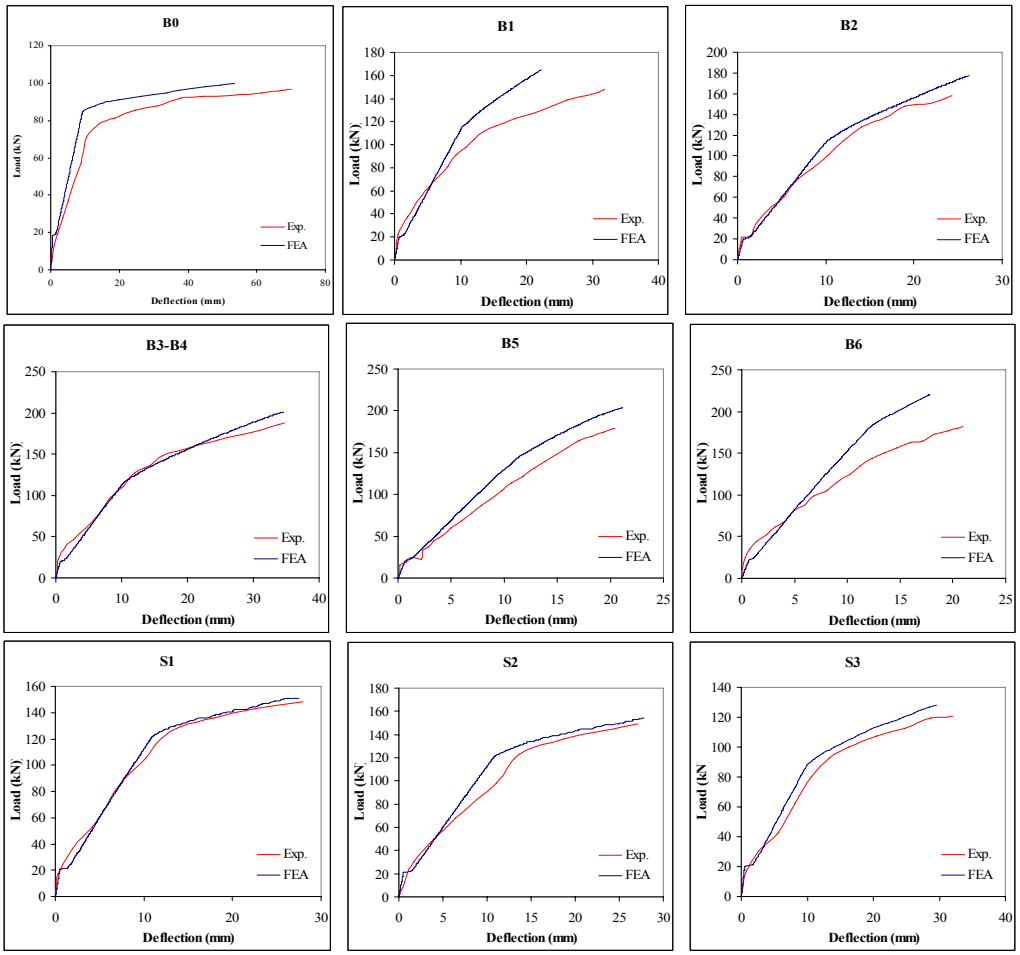

Figure 2: Experimental and numerical load–deflection curves.

4.2 Comparison of CFRP Strains

The strains in the CFRP obtained through FEA and the ACI 440 predictions are tabulated in Table 3. The MV of the strains in the CFRP obtained through FEA to the ACI 440 predictions and the SD are 1.11 and 0.18, respectively. It is observed that the results of FEA agree with the strains predicted using the ACI 440 equations.

For B series beams, the effects of number of plies and distance from the end of CFRP to the nearest support on the strains in the CFRP and the load-capacity of the beam were compared. It is observed that increasing the distance from the end of CFRP to the nearest support from 2134 mm (B1 beam) to 2286 mm (B2 beam) and 2744 mm (B3-4 beams) increases the ultimate strain by 16% and 52%, respectively (Table 4).

It is found that the strain in the CFRP of B5 beam consisted of 2Φ16 tensile reinforcement (0.00521) is greater than that of B6 beam consisted of 3Φ16 tensile reinforcement (0.00431). Since ACI 440 equations do not consider tensile reinforcement, the same value (0.00469) is predicted for both beams using ACI 440 equations (Table 4).

Beam	ε_{FEA} (1)	$\varepsilon_{fe,ACI440}$ (2)	(1)/(2)
B1	0.00637	0.00663	0.96
B2	0.00745	0.00663	1.12
B3-4	0.00973	0.00663	1.47
B5	0.00521	0.00469	1.11
B6	0.00431	0.00469	0.92
S1	0.01335	0.01182	1.13
S2	0.01299	0.01182	1.10
S3	0.01333	0.01182	1.13
		MV	1.12
		SD	0.16

Table 4: CFRP maximum strains.

5 Conclusions

On the basis of results obtained in this study, the following conclusions are drawn:

As the tensile reinforcement ratio increases, the strain in the CFRP decreases. Since ACI 440 equations do not consider tensile reinforcement, the same value is predicted for the beams with different tensile reinforcement ratios using the ACI 440 equations. It can be suggested that tensile reinforcement ratio should be considered in the calculation of the ultimate strains in FRP according to ACI 440.

As the distance from the end of CFRP to the nearest support decreases, the load-carrying capacity increases. Similarly, mid-span deflection increases with the distance from the end of CFRP to the nearest support (B1, B2, B3-4 beams).

It can be observed from the load-deflection curves that the load-carrying capacity increases with the number of plies. However, increasing the number of plies decreases the mid-span deflection. Therefore, it can be stated that the ultimate flexural strength of an RC beam strengthened by CFRP is directly proportional with the number of plies, while the ductility of the beam is inversely proportional with the number of plies.

References

[1] ACI Committee 440, “Guide for the Design and Construction of Externally Bonded FRP Systems for Strengthening Concrete Structures (ACI 440.2R-08)”, ACI, Miami, USA, 2008.

[2] M. N. Fardis, H. Khalili, “Concrete Encased in Fiberglass Reinforced Plastic”, ACI Journal Proceedings, 78(6), 440-446, 1981.

[3] R. Wolf, H. J. Miessler, “HLV-Spannglieder in der Praxis,” Erfahrungen Mit Glasfaserverbundstaben, Beton, 2, 47-51, 1989.

[4] U. Meier, “Bridge Repair with High Performance Composite Materials”, Material und Technik, 4, 125-128, 1987.

[5] F. S. Rostasy, 1987, "Bonding of Steel and GFRP Plates in the Area of Coupling Joints. Talbrucke Kattenbusch", Research Report No. 3126/1429, Federal Institute for Materials Testing, Braunschweig, Germany, 1987
[6] H Katsumata, Y. Kobatake, T. Takeda, "A Study on the Strengthening with Carbon Fiber for Earthquake-Resistant Capacity of Existing Concrete Columns", U.S.-Japan Panel on Wind and Seismic Effects, U.S.-Japan Cooperative Program in Natural Resources, Tsukuba, Japan, 1816-1823, 1987.
[7] U. Meier, H. Kaiser, "Strengthening of Structures with CFRP Laminates", Advanced Composite Materials in Civil Engineering Structures, ASCE Specialty Conference, 224-232, 1991.
[8] P. Ritchie, D. Thomas, L. Lu, G. Conneley, "External Reinforcement of Concrete Beams Using Fiber Reinforced Plastics", ACI Structural Journal, 88(4), 490-500, 1991.
[9] A. Sharif, G. Al-Sulaimani, I. Basunbul, M. Baluch, B. Ghaleb, "Strengthening of Initially Loaded Reinforced Concrete Beams Using FRP Plates", ACI Structural Journal, 91(2), 160-168, 1994.
[10] ANSYS 11.0, Theory Reference Manual, 2010.
[11] A. E. Demirer, "Finite Element Plastic Analyses of Reinforced Concrete Beams Strengthened by Fiber Reinforced Polymers", Ms Thesis, Yıldız Technical University, Istanbul, 2011 [in Turkish].
[12] ACI Committee 318, Building code requirements for structural concrete (ACI 318M–08) and commentary, ACI, Farmington Hills, MI, 473p., 2008.
[13] G. Arslan, F. Sevük, İ. Ekiz, "Steel Plate Contribution to Load Carrying Capacity of Retrofitted RC Beams", Construction and Building Materials, 22(3), 143-153, 2008.
[14] J. B. Mander, M.J.N. Priestley, R. Park, "Theoretical Stress-Strain Model for Confined Concrete", J Struct Eng (ASCE), 114(8), 1804-1826, 1988.
[15] Eurocode 2. Design of Concrete Structures, Part 1–1. General rules and rules for buildings, EN 1992–1–1. European Committee for Standardization. 2004.
[16] Concrete Society Technical (CST) Report 49, "Design guidance for high strength concrete", UK, 168 p., 1998.
[17] Y. Dong, M. Zhao, F. Ansari, "Failure Characteristics of Reinforced Concrete Beams Repaired With CFRP Composites", ICCI'02, California, 126-40, 2002
[18] H. Pham, R. Al-Mahaidi, "Experimental Investigation into Flexural Retrofitting of Reinforced Concrete Bridge Beams Using FRP Composites", 12th International Conference on Composite Structures, 66, 617-625, 2004.